6402 *Biochemistry* **2009,** *48,* 6402–6411
DOI: 10.1021/bi900655f

BIOCHEMISTRY
including biophysical chemistry & molecular biology
Article

Structural Bioinformatics-Based Prediction of Exceptional Selectivity of p38 MAP Kinase Inhibitor PH-797804[†,‡]

Li Xing,*[,§] Huey S. Shieh,[§] Shaun R. Selness,[∥] Rajesh V. Devraj,[∥] John K. Walker,[∥] Balekudru Devadas,[∥] Heidi R. Hope,[⊥] Robert P. Compton,[⊥] John F. Schindler,[⊥] Jeffrey L. Hirsch,[⊥] Alan G. Benson,[∥,] Ravi G. Kurumbail,[§] Roderick A. Stegeman,[§] Jennifer M. Williams,[§] Richard M. Broadus,[⊥] Zara Walden,[⊥] and Joseph B. Monahan[⊥]

[§]*Structural and Computational Chemistry and* [∥]*Medicinal Chemistry and* [⊥]*Discovery Biology, St. Louis Laboratories, Pfizer Global Research and Development, 700 Chesterfield Parkway West, Chesterfield, Missouri 63017*
Current address: Pharmaceutical Products, Covidien, 675 McDonnell Blvd., Hazelwood, MO 63042.

Received April 16, 2009; Revised Manuscript Received June 3, 2009

ABSTRACT: PH-797804 is a diarylpyridinone inhibitor of p38α mitogen-activated protein (MAP) kinase derived from a racemic mixture as the more potent atropisomer (a*S*), first proposed by molecular modeling and subsequently confirmed by experiments. On the basis of structural comparison with a different biaryl pyrazole template and supported by dozens of high-resolution crystal structures of p38α inhibitor complexes, PH-797804 is predicted to possess a high level of specificity across the broad human kinase genome. We used a structural bioinformatics approach to identify two selectivity elements encoded by the TXXXG sequence motif on the p38α kinase hinge: (i) Thr106 that serves as the gatekeeper to the buried hydrophobic pocket occupied by 2,4-difluorophenyl of PH-797804 and (ii) the bidentate hydrogen bonds formed by the pyridinone moiety with the kinase hinge requiring an induced 180° rotation of the Met109−Gly110 peptide bond. The peptide flip occurs in p38α kinase due to the critical glycine residue marked by its conformational flexibility. Kinome-wide sequence mining revealed rare presentation of the selectivity motif. Corroboratively, PH-797804 exhibited exceptionally high specificity against MAP kinases and the related kinases. No cross-reactivity was observed in large panels of kinase screens (selectivity ratio of > 500-fold). In cellular assays, PH-797804 demonstrated superior potency and selectivity consistent with the biochemical measurements. PH-797804 has met safety criteria in human phase I studies and is under clinical development for several inflammatory conditions. Understanding the rationale for selectivity at the molecular level helps elucidate the biological function and design of specific p38α kinase inhibitors.

p38α kinase is a key enzyme of the mitogen-activated protein kinase (MAP)[1] family that regulates the production and downstream signaling of inflammatory cytokines such as tumor necrosis factor-α (TNFα) and interleukins IL-1*β*, IL-6, and IL-8 (*1*−*3*). Evidence has been generated in both animal models and human studies that supports a role for TNFα and IL-1 in the pathogenesis of rheumatoid arthritis (RA) (*4*−*8*), an aggressive autoimmune disease involving complex interactions among T cells, macrophages, and other immune cells (*9*−*11*). By inhibiting the production of TNFα as well as signaling via multiple cytokines, p38α kinase inhibitors aim to disarm the proinflammatory mediators whose functions perpetuate the severity and chronicity of RA. Selective inhibitors of p38α kinase have been shown to block the production and activity of inflammatory cytokines and have demonstrated prominent efficacy in animal models of acute inflammation and arthritis (*12*−*15*).

Structural information of p38α kinase is rich with more than 50 published structures generated by X-ray crystallography over the past decades. Besides a few apo, unphosphorylated protein forms (*16*, *17*), most of the three-dimensional structures are binary complexes of p38α kinase and small molecule inhibitors that compete for binding with cellular ATP (*18*−*25*). The kinase hinge recognition predominantly involves a hydrogen bond with the Met109 backbone NH group. Some inhibitors engage an additional hydrogen bond with the upstream residue His107 via its backbone carbonyl, strictly resembling the donor−acceptor pattern of nucleoside interaction of ATP (*26*). A unique characteristic of the p38α hinge interaction resides in its potential for inducing a flipped conformation of the peptide bond connecting Met109 and Gly110. Binding to the flipped peptide conformation

[†]These studies were sponsored by Pfizer Inc.
[‡]The atomic coordinates and structure factors have been deposited in the Protein Data Bank as entries 3HL7 and 3HLL.
*To whom correspondence should be addressed. Telephone: (636) 247-5466. Fax: (636) 247-7607. E-mail: li.xing@pfizer.com.
[1]Abbreviations: MAP, mitogen-activated protein; MAPK, mitogen-activated protein kinase; RA, rheumatoid arthritis; PDB, Protein Data Bank; TNFα, tumor necrosis factor-α; DFT, density functional theory.

 Published on Web 06/04/2009

was reported for a number of inhibitor classes structurally related to quinazolinone (*18*, *23*, *27*, *28*).

In addition to the catalytically active conformations, the DFG-out arrangement constitutes one of the frequently encountered inactive kinase conformations (*29*, *30*). When specific classes of inhibitor molecules bind, the conserved Asp-Phe-Gly (DFG) motif at the beginning of the activation loop rotates out of the ATP site, creating a new pocket that is inaccessible in the active kinase conformation. By exploiting the induced pocket, submicromolar p38α kinase inhibitors were achieved sparing the conventional hinge interaction entirely (*26*). Since a limited number of kinases have been demonstrated to adopt the DFG-out conformation, binding to such conformational states is believed to lead to better kinase selectivity. For some known kinase inhibitors, this was the structural basis for their minimal off-target kinome crossover (*31*, *32*).

Here we report a novel and orally active p38α kinase inhibitor, PH-797804, its high potency ($K_i = 5.8 \pm 0.3$ nM), and, more importantly, its superb kinase selectivity. By comparing binding interactions with different chemical series elucidated by crystal structures, we show that PH-797804 achieves its selectivity not by inducing the inactive kinase conformations but rather by combining distinctive interactions with the hinge and the unique hydrophobic pocket of p38α kinase. The exceptional selectivity of PH-797804 is substantiated by results from the enzymatic inhibition of other MAP kinases, the large panels of kinase screening assays, and the cellular determination of phosphorylation events in the p38α activation pathway. Consistent with in vitro evaluations, PH-797804 has been proven to be safe and well-tolerated in phase I clinical trials. It is currently under phase II development for the treatment of several inflammatory diseases (*33*).

EXPERIMENTAL PROCEDURES

X-ray Crystallography. Human p38α kinase was expressed and purified following protocols described previously (*16*−*20*). Crystals of p38α kinase complexed with inhibitors were grown by a two-step sitting drop method of vapor diffusion. Purified p38α kinase was concentrated to 6 mg/mL in 50 mM HEPES (pH 7.5), 50 mM NaCl, 5% glycerol, and 2 mM DTT, and then a weak p38α kinase binder, normally a diarylpyrazole compound, such as 2-fluoro-4-[4-(4-fluorophenyl)-1*H*-pyrazol-3-yl]pyridine in this case, was added to a final concentration of 1 mM. The p38α kinase−diarylpyrazole complex solution was mixed 1:1 with a reservoir solution containing 14−26% PEG 3000, 5−80 mM $CaCl_2$, and 50 mM CHES (pH 9.0) in a Q-plate sitting drop crystallization plate. Prism-shaped crystals grew at ambient temperature to a maximum size of 0.4 mm × 0.2 mm × 0.2 mm over a period of 1−2 weeks.

Cocrystals of the p38α−diarylpyrazole complex were used as "surrogate native" crystals for soaking experiments. The diarylpyrazole molecule was displaced at the ATP-binding site of p38α kinase by using an excess of PH-797804 in the soaking experiments. The p38α kinase−diarylpyrazole cocrystals were stabilized in 24% PEG 3000, 80 mM $CaCl_2$, 50 mM CHES (pH 9.0), and 1 mM PH-797804. Soaking experiments were conducted over a period of at least 24 h at room temperature.

Diffraction data were collected on a MAR-ccd detector, using synchrotron X-rays generated at beamline 17BM in the facilities of the Industrial Macromolecular Crystallography Association Collaborative Access Team (IMCA-CAT) at the Advanced Photon Source (Argonne National Laboratory, Argonne, IL). A crystal of the p38α kinase complex with PH-797804 was transferred to a small loop from the soak solution cryoprotected with 20% ethylene glycol and flash-frozen in a bath of liquid nitrogen. Each image of the diffraction data was recorded with a ϕ step of 0.7° for 2 s. The diffraction data were 99.6% complete with an R_{sym} of 5.3% to 1.95 Å resolution. A total of 27860 unique reflections were derived from 258 images with a redundancy of 6.9-fold. The crystal belongs to space group $P2_12_12_1$ with the following unit cell dimensions: $a = 65.114$ Å, $b = 74.645$ Å, and $c = 77.066$ Å. Data reduction and processing were performed with the HKL2000 suite of programs.

The crystal structure of the complex was determined by difference Fourier methods using the known structure of p38α kinase. Electron density maps were calculated after a few cycles of rigid body, positional, and *B* factor refinement. Inhibitors were modeled into the electron density using O and further refined using X-plor. The structure of the PH-797804 complex has been refined to 1.95 Å resolution with an R_{work} of 24.5% (R_{free} = 29.9%) and good stereochemistry (root-mean-square deviation from ideality of 0.007 Å in bond lengths and 1.2° in bond angles).

MAP Kinase Inhibition Assays. p38α kinase activity was determined by monitoring the phosphorylation of epidermal growth factor receptor peptide (EGFRP) by p38α kinase in the presence of [γ-^{33}P]ATP and ATP using a resin capture technique. The unreacted [γ-^{33}P]ATP is separated from phosphorylated EGFRP using an anion-exchange resin, AG 1X8. p38α kinase activity is quantified through evaluation of an aliquot of ^{33}P-labeled EGFRP in the presence of scintillation cocktail. The assay was performed in the presence of 10% DMSO and was conducted for 30 min at room temperature. A K_i value for PH-797804 was obtained using the Dowex assay. For these determinations, ATP/[γ-^{33}P]ATP was used as the varied substrate and the peptide (EGFRP) was tested at a single fixed concentration. The inhibition data were fit to a competitive inhibition model using GraFit version 4.0.

The resin capture kinase assay was utilized to evaluate the potency of PH-797804 against several other kinases and was based on the phosphorylation of peptide or protein substrates by activated kinases in the presence of 0.2 μM ATP/[γ-^{33}P]ATP. Kinases were tested for their sensitivity to inhibition in 50 μL reaction volumes containing 10 mM magnesium acetate, 4% glycerol, 0.4% bovine serum albumin, 0.4 mM dithiothreitol (DTT), unlabeled ATP, 1 mM Na_3VO_4, and [γ-^{33}P]ATP at pH 7.5. Reactions were initiated by addition of activated kinase. Compounds were tested in 10-fold serial dilutions, beginning at 100 or 200 μM in a final DMSO concentration of 10%. Each concentration of inhibitor was tested in triplicate. Inhibition studies were conducted using ATP concentrations at the K_m (Michaelis−Menten constant) measured for the respective kinases and at a peptide substrate concentration 10-fold greater than the K_m as determined for each kinase. The reactions were allowed for each enzyme assay to proceed so that the conversion of substrate was kept at less than 30% of the total substrate. Following incubation for various time at room temperature, the kinase reactions were stopped by addition of 150 μL of AG 1X8 resin in 900 mM sodium formate buffer (pH 3.0) (1 volume of resin to 2 volumes of buffer). At pH 3.0, the AG 1X8 ion-exchange resin selectively binds ATP, leaving inorganic phosphate and phosphorylated substrate in solution. The suspension was mixed three times and allowed to settle; 50 μL of head volume was transferred from the reaction wells

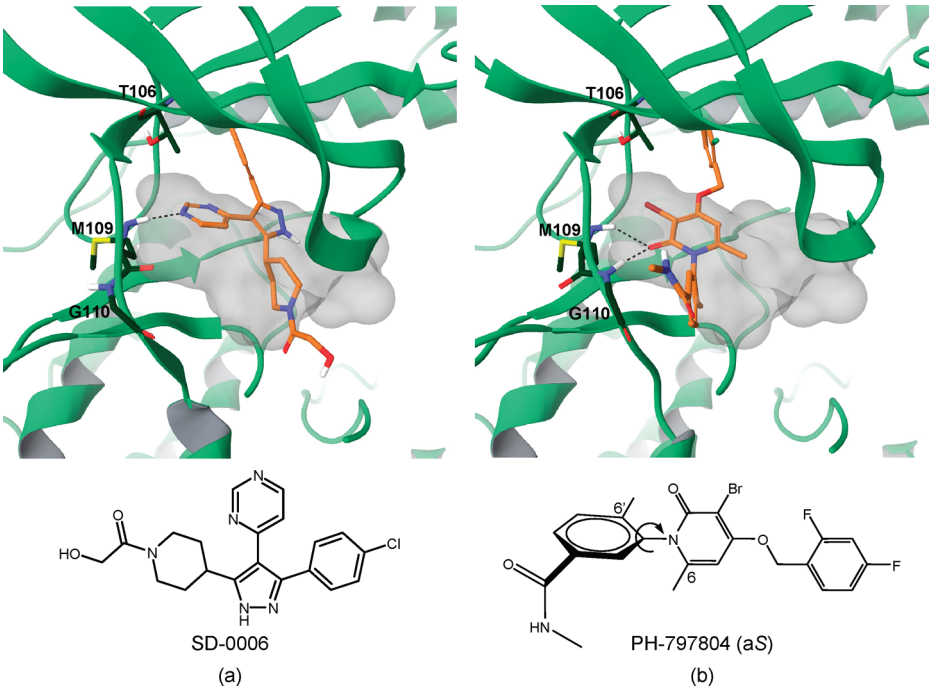

FIGURE 1: Molecular structures of p38α inhibitors SD-0006 (a) and PH-797804 (b) and their binding interactions illustrated by crystal costructures with the p38α kinase domain. Hydrogen bonds are drawn as dotted lines. The ATP binding site is delineated by the molecular surface of AMP-PNP extracted from the p38γ crystal structure (PDB entry 1CM8).

to Microlite-2 plates. Next, 150 μL of Microscint-40 was added to each well of the Microlite-2 plate. The plate was sealed, mixed, and counted using a Packard TopCount NXT plate reader. IC_{50} values were calculated using a four-parameter logistic model. The Myt-1 kinase assay was run at K_m for ATP at 50 μM, myelin basic protein (MBP) substrate at 1 mM, and 50% pure Myt-1 at 30 ng/μL, in resin capture format.

Kinase Selectivity Screen. The panel of biochemical kinase assays was run in a 384-well streptavidin capture (Flashplate) format. The reactions were conducted in polypropylene plates where the kinase was incubated in the presence of a specific biotinylated peptide and a mix of both unlabeled ATP and [γ-^{33}P] ATP (at concentrations of ATP K_m for each kinase). The reaction was stopped via EDTA chelation, and the reaction mixture was transferred into the Flashplate for readout. The activity of the kinase was measured by the incorporation of ^{33}P onto the biotinylated peptide, which was captured on the streptavidin-coated plate and brought into the proximity of the scintillant. The signal was measured as light output. Compound activity was measured as the percent inhibition of the total signal based upon the control wells. Careful statistical monitoring of each plate for signal window and *Z* values allowed the data to be reported with a high degree of confidence.

Cellular Selectivity Assays. The U937 human premonocytic cell line was obtained from American type Culture Collection (Rockville, MD). U937 cells were grown in RPMI 1640 (Gibco, Carlsbad, CA) with glutamine, penicillin/streptomycin (10 units/mL) (Gibco), and 10% heat-inactivated fetal bovine serum (Gibco). Cells were differentiated to a monocyte/macrophage phenotype with the addition of phorbol 12-myristate 13-acetate (PMA) (Sigma Chemical Co., St. Louis, MO) (20 ng/mL, 24 h), washed with Dulbecco's phosphate-buffered saline (D-PBS) (Gibco), and incubated in complete medium for 24 h at 37 °C. Following recovery, the cells were scraped, counted, replated in complete medium in accordance with the experimental design, and incubated for an additional 24 h at 37 °C prior to stimulation with LPS (*Escherichia coli* serotype 011:B4) as described below.

Differentiated U937 cells, pretreated with or without inhibitors for 1 h, were stimulated with LPS (0.1 μg/mL) for a period of 30 min followed by a rapid lysis in RIPA buffer (1× PBS, 1% NP40, 0.5% sodium deoxycholate, and 0.1% SDS) containing sodium orthovanadate (1 mM) and PMSF (phenylmethanesulfonyl fluoride) (Sigma Chemical) (500 μM) for Western blot analysis.

U937 cell RIPA lysates were evaluated for p38α kinase, JNK, ERK, and c-Jun phosphorylation (activation) by Western blotting using isoform selective antibodies or phospho-specific antibodies [phospho-p38 from Invitrogen (Carlsbad, CA), total JNK from Promega (Madison, WI), phospho-Hsp27 generated in house, and all other antibodies from Santa Cruz Biotechnology (Santa Cruz, CA)].

RESULTS AND DISCUSSION

PH-797804 (aS) Is the More Potent Atropisomer of a Racemic Pair. Because of the steric bulk of the pyridinone carbonyl and the 6,6′-methyl substituents of PH-797804, the torsional rotation about the bond connecting the pyridinone and the *N*-phenyl ring is hindered (Figure 1). This gives rise to discrete conformational spaces of the *N*-phenyl pyridinone group and as a result two atropic isomers that do not interconvert under ambient conditions. The existence of the atropisomers was first discovered by molecular modeling which revealed a remarkably high rotational energy barrier around the *N*-phenyl dihedral (e.g., >25 kcal/mol). Modeling studies further predicted that the two isomers should differ in their binding affinity for p38α kinase, based on the analysis that whereas the atropic *S* isomer (a*S*) binds favorably to p38α kinase, the opposite a*R* isomer would incur significant steric interference between the methyl amide moiety derived from the *N*-phenyl ring and the amino acids Asp112 and Asn115 of the p38α protein. Subsequently,

two isomers were identified and separated by reverse phase chiral chromatography. IC_{50} values from the p38α enzyme assay confirmed that one atropisomer is >100-fold more potent than the other. It was ultimately resolved by small molecule X-ray diffraction that the more potent atropisomer (PH-797804) is the a*S* isomer of the racemic pair. Extensive pharmacological characterization supports the idea that PH-797804 carries most activity both in vitro and in vivo, and it has a stability profile that is compatible with oral formulation and delivery options.

Binding of PH-797804 to p38α Kinase Induces a Conformational Change in the Protein Backbone. Crystal structures of the earlier class of p38α kinase inhibitors based on the biaryl pyrazole template have revealed a number of binding elements represented by SD-0006 (Figure 1a) (*34*). In comparison, PH-797804 not only retained the conserved elements of binding to p38α kinase in the conventional kinase inhibition mode but also demonstrated unique structural features (Figure 1b). Both inhibitor classes compete for the ATP binding site of p38α kinase located at the folding cleft between the N- and C-terminal lobes. Comparison of the crystal structures of the p38α−inhibitor complex with the p38γ−AMP-PNP system suggests that the binding of the pyridinone moiety of PH-797804 partially overlaps with the adenine of ATP, as does the pyrimidine group of SD-0006. Besides, the inhibitors occupy a unique aryl pocket that is divergent from phosphate binding of ATP. Consistent with the chlorophenyl interaction of SD-0006, the 2,4-difluorophenyl group of PH-797804 is encapsulated in a lipophilic pocket of p38α kinase, completely shielded from the solvent. The contour of the pocket appears to be thoroughly complementary to the halogenated phenyl ring of the inhibitor, from which a major portion of the binding free energy is derived as suggested by modeling studies. This hydrophobic pocket, unoccupied by ATP, appears to be the anchor point for the positioning and orientation of p38α kinase inhibitors of diverse chemical scaffolds. The gatekeeper residue Thr106, sitting at the entrance thus controlling the access to the pocket, therefore is of essential importance to the binding affinity of p38α inhibitors.

For kinase hinge recognition, the pyrimidine nitrogen of SD-0006 receives one hydrogen bond from the backbone of Met109, which is in a consistent conformation with the apo p38α structure. On the other hand, the pyridinone carbonyl oxygen of PH-797804 forms two hydrogen bonds, one with the amide nitrogen of Met109 and the other with the backbone NH group of Gly110. To achieve the suitable geometry for the second hydrogen bond interaction, the amide bond connecting Met109 and Gly110 undergoes a backbone flip, completely reversing the orientations of the carbonyl and amino moieties from their apo conformations. In concert with the backbone flip of the kinase hinge, the pyridinone of PH-797804 is positioned further downstream compared to the pyrimidine of SD-0006, resulting in equal distances of the bidentate hydrogen bonds with the amino groups of Met109 and Gly110 (ca. 3.0 Å between heavy atoms). This bidentate hydrogen bond formation utilizes the two lone pairs of the participating carbonyl oxygen atom, which compares to the single lone pair of the pyrimidine nitrogen of SD-0006. The enhanced binding affinity derived from the additional hydrogen bond is reflected in the enzymatic potencies of these two classes of inhibitors; e.g., PH-797804 is ~4-fold more potent than SD-0006 against p38α kinase (Table 1).

In PH-797804, the 6,6′-methyl substituents and the pyridinone carbonyl together render the *N*-phenyl ring orthogonal to the pyridinone core. The density functional theory (DFT) calculation yielded a torsion angle of 76.2° upon full optimization of PH-797804 (B3LYP/3-21G*), which suggests that in the minimum-energy state, the 6′-methyl derived from the *N*-phenyl ring is tilted slightly toward the pyridinone carbonyl. Upon binding to p38α kinase, PH-797804 demonstrates a dihedral angle of 103.2°, with the 6′-methyl tilting toward the 6-methyl off the pyridinone. The orthogonality of the *N*-phenyl pyridinone appears to be instrumental to the inhibitory activity against p38α kinase, which we rationalize in two aspects of enthalpic optimization. First, the bidentate hinge hydrogen bonds are strengthened, primarily by the enriched electron density on the carbonyl oxygen as a result of the minimized aromatic conjugation, and additionally by the sterically exposed hydrogen bond acceptor atom. Second, the orthogonal conformation facilitates the stacking between the *N*-phenyl ring of PH-797804 and the peptide bond connecting Gly110 and Ala111. X-ray crystal structures indicate that such stacking interaction is highly conserved for the pyridinone compound class. Because the free conformation of the *N*-phenyl pyridinone group is constrained in a manner similar to that of its bound state, the conformational entropy loss upon binding is diminished. As a result, a favorable gain in the binding free energy is achieved and reflected in the high affinity of PH-797804 for p38α.

Table 1: Enzyme Activities of SD-0006 and PH-797804

	sequence identity of the kinase domain and p38α kinase (%)	gatekeeping residue	SD-0006[a]	PH-797804[b]
p38α	100	T	0.023 μM[c]	0.0058 μM[c]
p38β	78	T	0.444 μM[c]	0.040 μM[c]
p38γ	65	M	>100 μM	>200 μM
p38δ	65	M	>100 μM	>200 μM
JNK1	50	M	38 μM	>200 μM
JNK2	53	M	2.2 μM	>200 μM
JNK3	51	M	7.7 μM	>200 μM
ERK2	50	Q	>30 μM	>200 μM
Myt-1	23	T	not tested	>10 μM
CKIα	29	M	98%	>10 μM
CKIδ	28	M	94%	>10 μM
EGFR	27	T	70%	>10 μM
PKA	27	M	62%	>10 μM
c-RAF	27	T	77%	>10 μM

[a] Numbers listed are either IC_{50} values (micromolar) or percent inhibition at 10 μM. [b] Additionally, IC_{50} values for PH-797804 against the following targets have been determined to be greater than 200 μM (unless specified): CDK2, ERK2, IKK1, IKK2, IKKi, MAPKAP2, MAPKAP3, MKK7 (>100μM), MNK, MSK (>164 μM), PRAK, RSK2, and TBK1. [c] K_i values.

The Flipped Peptide Conformation Can Be Accessed by Only a Glycine Residue. The conformational space of a polypeptide is best investigated by a Ramachandran diagram (*35*, *36*). The two-dimensional ψ and ϕ maps were generated for Met109 and Gly110 from a large number of p38α kinase crystal structures (Figure 2). Distinctly, the backbone conformations of the residues cluster into two regions on the Ramachandran diagram: one cluster represents the apo p38α kinase conformations, and the other depicts the induced peptide bond flip upon binding of the pyridinone inhibitor class. It is evident that binding of SD-0006 preserves the unperturbed apoprotein state.

Without exception, compounds of the pyridinone class bind to the peptide-flipped conformation of p38α, in which the ψ of Met109 and ϕ of Gly110 undergo simultaneous rotations of 180°

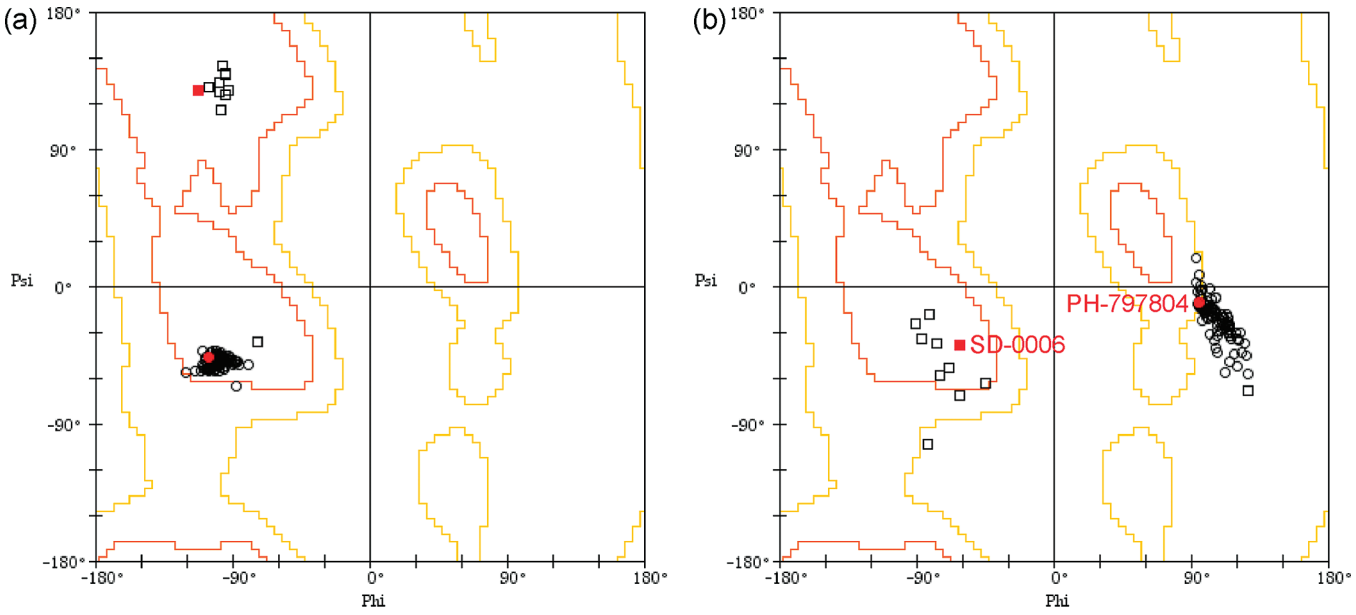

FIGURE 2: Ramachandran diagram of p38α kinase Met109 (a) and Gly110 (b). Squares represent 10 p38α crystal structures that are apo in both the ATP and substrate binding sites from the PDB. Circles represent 84 binary complexes of p38α kinase and congeneric inhibitors of the pyridinone class. Highlighted in red are SD-0006 (red square) and PH-797804 (red circle). The areas inside the red contour, between the red and yellow contours, and outside the yellow contour delineate favored, disfavored but allowed, and disallowed regions, respectively.

from their apo states, whereas the Met109 ϕ and Gly110 ψ torsions are more or less preserved. Such concerted inversion of the two dihedral angles gives rise to the flipped amide bond connecting Met109 and Gly110, characteristic of ligand binding of PH-797804 and the pyridinone class of p38α inhibitors.

On the Ramachandran diagram of Met109, both the native and induced conformations reside in the allowed region. However, it is noted that for Gly110, although the apo states are normally accessible, the flipped conformations are primarily forbidden for other amino acids that bear a side chain. In other words, the conformational states required for the bidentate hydrogen bond between PH-797804 and the hinge can be accessed by only a glycine residue at position 110 of p38α kinase. Reported site-directed mutagenesis results support the glycine prerequisite for the flipped Met109-Gly110 peptide conformation (*18*). For quinazolinone and related classes of inhibitors, mutations of Gly110 to alanine or aspartate resulted in a loss of inhibitory activity by ≥1 order of magnitude.

Upon surveying the apo p38α kinase structures, we found one exception in which the Met109−Gly110 backbone torsions resemble the inhibitor-induced conformation (PDB entry 1R39). This could be due to its moderate resolution of 2.3 Å, as our experience suggested that the native and the induced conformations are not readily distinguishable unless for high crystal resolutions.

The TXXXG Motif Imparts Kinase Selectivity of PH-797804. Two characteristics summarize the binding interactions of PH-797804 with p38α kinase: (i) the hydrophobic encapsulation in a pocket that is distinct from phosphate binding of ATP, gated by Thr106, and (ii) the bidentate hydrogen bonds with Met109 and Gly110 requiring a peptide bond flip into the conformation that is only available for a glycine residue. It is hence concluded that the TXXXG sequence motif highlights the important and unique interaction elements utilized by the PH-797804 inhibitor class upon their binding to p38α kinase. Understanding the implication of such structural features to the desirable potency and specificity that can be achieved by a druglike small molecule has paramount importance for targeting p38α kinase as a therapy for many chronic autoimmune disorders.

Structural comparison with a closely related homologue, e.g., p38γ kinase which has a methionine in place of Thr106, revealed that amino acids of side chains larger than threonine could significantly block the access to the aryl pocket. The importance of Thr106 is also suggested by a number of site-directed mutagenesis studies (*37*−*39*), while mutations of Thr106 to glutamine or methionine rendered significant loss of activity for a set of potent p38α inhibitors (*39*). Given its gatekeeping role, we speculate that amino acids of side chains similar to or smaller than threonine in size would not temper the access to the aryl pocket and thus could be suitable replacements for Thr106. Such equivalent mutations conceivably include cysteine, serine, alanine, and glycine residues. It is therefore implicit that the TXXXG shorthand encompasses the additional four equivalents to the sequence of p38α from which it is derived.

We mined the TXXXG motif in the human genome consisting of 518 protein kinase complements (*40*) and plotted the sequence distribution profiles corresponding to Thr106 and Gly110 of p38α kinase in Figure 3. The analysis reveals that 99 kinases, or 20% of the kinome, have threonine or one of the equivalent replacements in the position of Thr106. On the other hand, 44 kinases share a glycine residue at the position corresponding to Gly110, which constitute 9% of the human kinase genome. The combined TXXXG motif, the hallmark interaction of PH-797804 and the pyridinone class it represents, is sparingly conserved by three kinases, specifically p38α, p38β, and Myt-1. p38β kinase is the closest structural homologue to p38α, sharing 75% overall sequence identity, and even higher in the ATP binding site (close to 90%). In general, p38β kinase exhibits an inhibition profile similar to that of p38α for a diverse set of compounds, including biaryl pyrazoles and pyridinones discussed herein (Table 1). Myt-1 is a mixed serine/threonine and tyrosine kinase upstream of CDKs. Its kinase domain is merely 23% identical to that of p38α in primary structure. Hence,

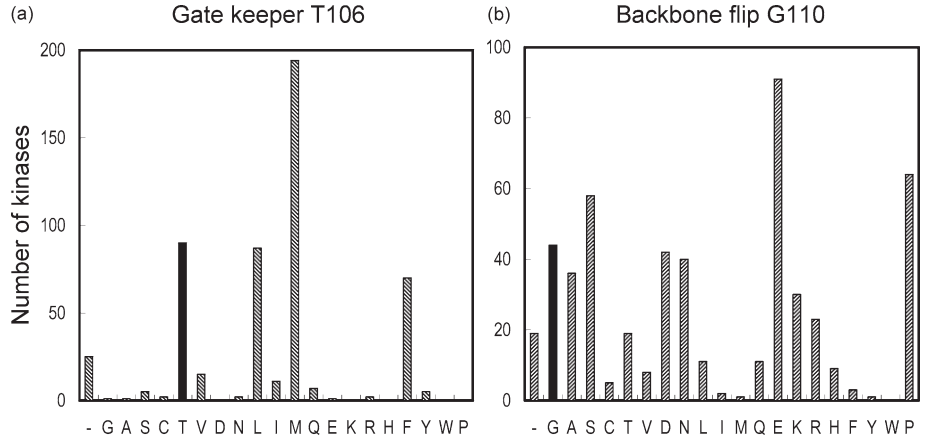

FIGURE 3: Amino acid frequencies of the human kinome at positions corresponding to p38α kinase Thr106 (a) and Gly110 (b). The filled bars represent frequencies of the threonine residue (a) and glycine residue (b). Amino acids on the *x*-axis are sorted approximately by the size of side chains, where a dash represents a gap.

we predicted PH-797804 would not crossover to Myt-1 due to divergent three-dimensional folds and active site compositions between p38α and Myt-1 kinases. In the next section, we report that PH-797804 is not active in the Myt-1 enzyme assay.

In summary, the TXXXG motif on the hinge of p38α kinase not only furnishes potent enzyme inhibition for the PH-797804 compound class but also provides the potential for a high degree of kinase selectivity. Bioinformatics mining of the human kinase genome uncovered only one protein target, p38*β* kinase specifically, that is likely to show cross reactivity with PH-797804. The pyridinone chemical class and its related variations, in comparison with the biaryl pyrazole class discussed herein, possess inherent specificity as a result of a unique combination of binding interactions with p38α kinase.

MAP Kinase Inhibitory Activities. Except for p38 α and *β* isoforms, other members of the MAP kinase family have different residues in positions of Thr106 and Gly110. Such structural differences render the PH-797804 compound class more selective than the SD-0006 chemotype for MAP kinases. Table 1 lists in comparison their activities against a number of human kinases that are structurally related to p38α. Four isoforms of p38 kinase have been identified: p38α, p38*β*, p38*γ*, and p38δ. With an enzymatic K_i of 5.8 nM, PH-797804 is 4-fold more potent than SD-0006 against the primary target, p38α kinase. Although both inhibitor classes typically avoid interactions with p38*γ* and p38δ, p38*β* kinase inhibition activity generally parallels that of p38α with an attenuated magnitude in potency. The potency shifts are typically in the range of 10−20-fold from p38α to p38*β* for both the biaryl heterocycle and the pyridinone classes.

As illustrated in Table 1, PH-797804 exhibits a high level of selectivity against JNK family kinases as projected from the bioinformatics analysis of the TXXXG motif. JNK kinases have conserved methionine and aspartate residues in place of Thr106 and Gly110 of p38α kinase. On the basis of the structural model, interaction with the hydrophobic pocket shall be impeded and the hydrogen bond with the hinge is attenuated for JNK kinases. The end result of the two contributing factors is the differentiated selectivity profile of the two chemical classes, represented by SD-0006 and PH-797804, respectively. Since SD-0006 does not engage in a hydrogen bond to Gly110, the threonine-to-methionine mutation alone is not sufficient to impart high specificity against the JNK family kinases.

Other tested kinases containing methionine in the position of Thr106 include CKIα, CKIδ, and PKA, against which SD-0006 also exhibits a higher degree of inhibition than PH-797804. The greater specificity of PH-797804 against EGFR and c-RAF is attributed to its additional interaction with Gly110 compared to SD-0006. Myt-1 emerged from our kinome mining as one of the three kinases that strictly conserves the TXXXG motif. Cross-reactivity is not anticipated for PH-797804 because of the remote evolutionary relationship between Myt-1 and p38α kinase. This is confirmed by a marginal inhibition of 14% at a concentration of PH-797804 of 10 *μ*M.

For more than a dozen kinases, including members of the MAP kinase family, PH-797804 consistently demonstrates a higher level of specificity than SD-0006, sparing the entire JNK family and a number of other important kinase targets that are inhibited by SD-0006. The superior selectivity of PH-797804 resides in its simultaneous engagement of the dual structural motifs manifested by the TXXXG sequence on the hinge of p38α kinase. Engaging only one interaction with either Thr106 or Gly110 is not adequate for a small molecule inhibitor to be selective against a large panel of kinases.

Kinase Selectivity Screens. PH-797804 was further tested against several kinase screening panels for its off-target activities. The kinase selectivity panels contain a large number of targets covering diverse kinase families, as indicated by the broad distribution over the kinase dendrogram (Figure S1 of the Supporting Information). In the first screening panel (Figure 4a), p38α kinase is completely inhibited at 1 and 10 *μ*M PH-797804, while none of the other kinases reach 20% inhibition. In the second kinase panel (Figure 4b), p38α kinase is completely inhibited at all three concentrations, and the rest of the inhibitions are less than 20%, with most under 10%. Of the kinases comprising the two aforementioned panels, 22 kinases are common in both. The consistent inhibition values produced by the two independent screens for the overlapping targets substantiate the high quality of the individual screens. In total, the two panels provide selectivity evaluation for 58 human kinases, in which PH-797804 was found to be completely selective with no off-target signal. The selectivity windows are greater than 500-fold compared with the primary target p38α kinase.

The requirement of the dual structural motifs is further supported by probing the in vitro screening results. Of the kinases

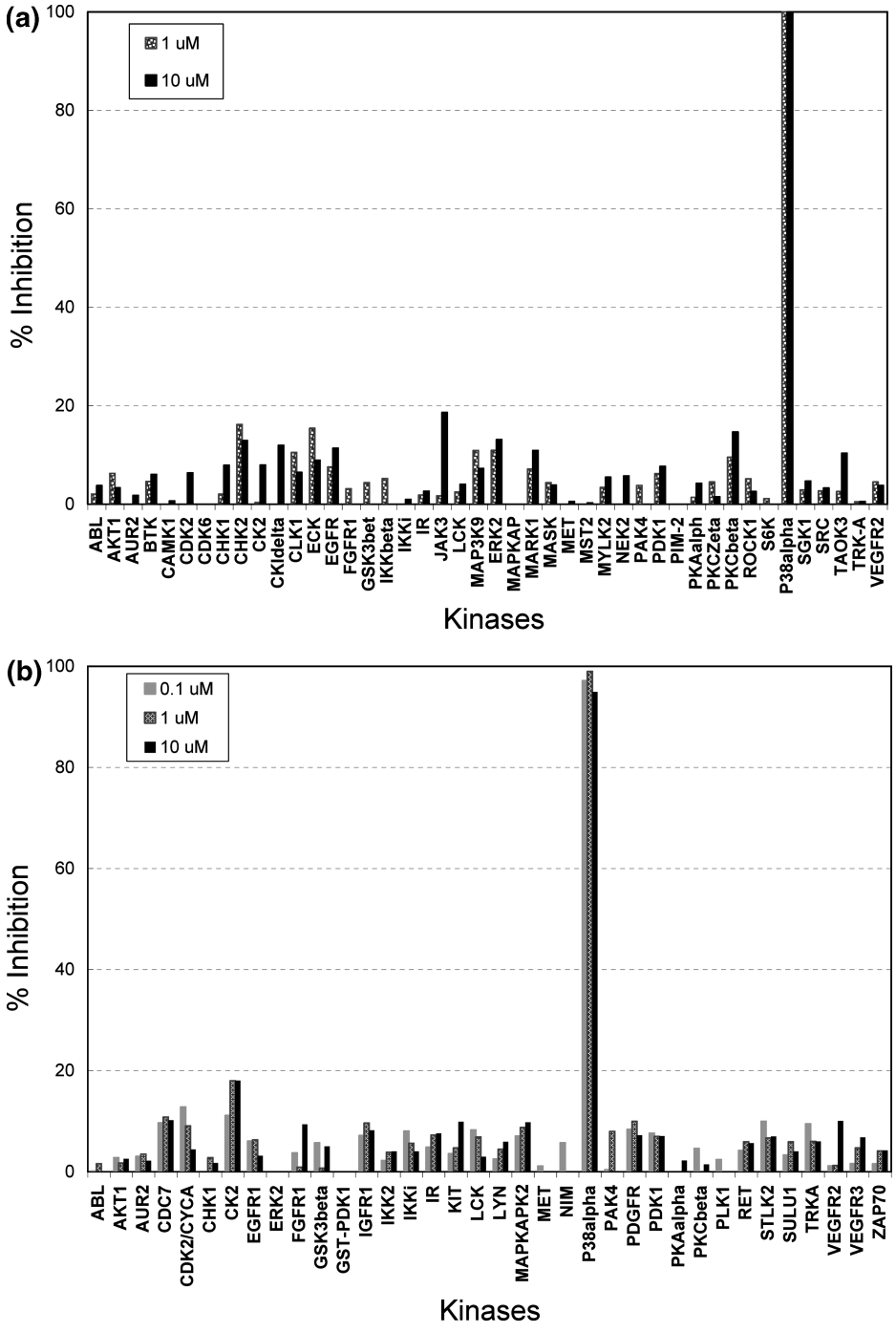

FIGURE 4: PH-797804 inhibition from two kinase selectivity screens. (a) A panel of 44 kinases. Each target is tested at two concentrations (1 and 10 μM) in duplicate. (b) A panel of 36 kinases. Each target is tested at three concentrations (0.1, 1, and 10 μM). Each data point represents the average of 12 measurements.

tested, approximately a dozen meet the single-motif criteria at either position Thr106 or Gly110. Tested kinases bearing equivalent residues in place of Thr106 are Abl, Fyn, Lck, Lyn, EGFR, PDGFR, HER2, and STLK. Indeed, they all strictly conserve Thr106, while mutations for Gly110 are widespread. On the other hand, representatives of Gly110 conservation are p38γ, ZAP70, and NIM1, which share a MXXXG pattern in their primary structures. At the highest screening concentration of 10 μM, PH-797804 demonstrated $<10\%$ inhibition against all aforementioned targets. The fact that PH-797804 does not inhibit such kinases satisfying either structural feature reinforces the dual-motif theory. The rare representation of the TXXXG hinge in the human kinome forms the basis of minimum off-target activity of PH-797804. Our early understanding and prediction of the exquisite selectivity of PH-797804 impart confidence in developing a highly selective p38α kinase inhibitor that could meet the safety criteria for chronic autoimmune indications.

Cellular Potency and Selectivity. For many kinases, inhibitor potency exhibited in a purified biochemical kinase assay does not directly transfer to the more complex and physiologically relevant cellular assay. The biochemical to cellular assay disconnect may be a result of several factors, including (i) high ATP levels in cells, (ii) cellular penetration, (iii) the nature of the protein construct utilized for the biochemical measurements, and (iv) the impact that cellular macromolecular complex formation, common with signal transduction kinases, has on the activity and

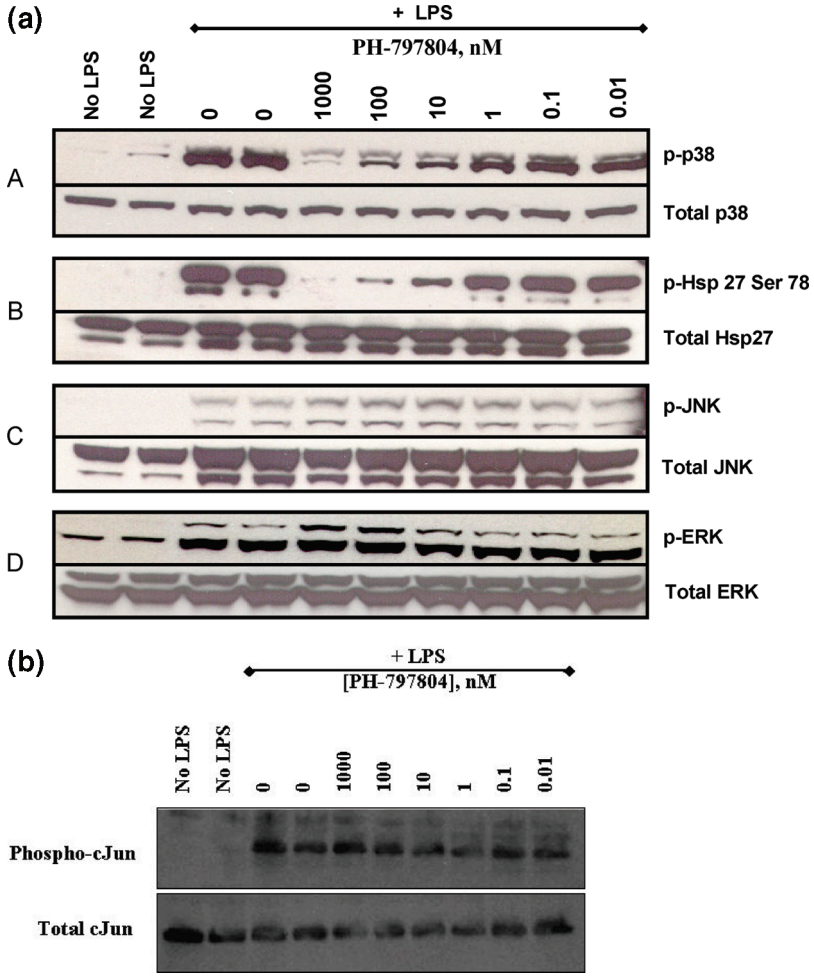

FIGURE 5: Cellular activity and selectivity of PH-797804. U937 cell lysates are evaluated for phosphorylation of MAP kinases by Western blotting using isoform selective antibodies or with phospho-specific antibodies: (a) phosphorylation of p38 kinase, JNK, and ERK and (b) phosphorylation of c-Jun.

structure of the target kinase. In an effort to evaluate the translatability of potency and selectivity of PH-797804 for p38α kinase between biochemical and cellular assays, the potency of the inhibitor was determined in the LPS-stimulated human promonocytic cell line, U937.

Panels A and B of Figure 5a demonstrate using Western blotting, that PH-797804 inhibits both p38 phosphorylation and the phosphorylation of the downstream substrate HSP-27 in a concentration-dependent manner with 50% inhibition observed between 1 and 10 nM, consistent with the value obtained in biochemical assays. These data suggest that PH-797804 binding to p38α kinase inhibits both its phosphorylation and activity, characteristics similar to those of previously described inhibitor classes (*41*, *42*). The result is also consistent with an earlier report that the kinase activity of p38 kinase is required for its own phosphorylation (*42*). Furthermore, a direct correlation exists between cellular and enzyme potency. Cellular selectivity was demonstrated against the other classes of MAP kinase enzymes JNK (Figure 5a, panel C) and ERK (Figure 5a, panel D). The lack of inhibition observed with PH-797804 for ERK and JNK suggests that the inhibitor does not have an impact on the phosphorylation of these two kinases or any kinases upstream in their respective pathways. The lack of an effect of PH-797804 on phosphorylation of c-Jun (Figure 5b) confirms the lack of inhibitory activity against JNK in this cellular system. Overall, the cellular potency and selectivity of PH-797804 correlate very well with the biochemical data and extend the observation of high target potency and selectivity.

Interestingly, inhibition of p38 upon LPS challenge appears to slightly increase the level of phosphorylation of ERK and JNK (Figure 5a), possibly due to a feedback control mechanism via their overlapping upstream kinases. For example, the TAK-1 binding protein TAB-1 regulates the activity of the MAPKKK, TAK-1. Phosphorylation of the TAB-1 protein by p38 MAPK results in a decrease in the activity of TAK-1 which, in turn, downregulates the MAPK signaling pathways, including ERK and JNK. In agreement with this mechanism, inhibition of TAB-1 phosphorylation by a p38 inhibitor results in an upregulation of TAK-1 activity (*43*). Similarly, in a p38α knockout study, excessive JNK activation was found after LPS challenge (*44*). To add to the dynamics of MAPK phosphorylation states, MAPK phosphohatase-1, a dual-specificity phosphatase that preferentially dephosphorylates p38 MAPK and JNK family members, is upregulated by stress-activated protein kinase cascades including p38 MAPK (*45*). Therefore, p38 kinase inhibitors could modulate the MAPK pathway via multiple regulatory and feedback mechanisms.

ACKNOWLEDGMENT

We thank Dr. Timothy Benson and the reviewers for insightful suggestions about the manuscript. L.X. thanks Joseph Moon for

his help in retrieving structural coordinates. Use of IMCA-CAT beamline 17-BM was supported by the Industrial Macromolecular Crystallography Association through the Center for Advanced Radiation Sources at the University of Chicago.

SUPPORTING INFORMATION AVAILABLE

Kinase selectivity panels contain representative members from each human kinase family, distributed broadly over the protein kinase dendrogram (Figure S1). This material is available free of charge via the Internet at http://pubs.acs.org.

REFERENCES

(1) Ridley, S. H., Sarsfield, S. J., Lee, J. C., Bigg, H. F., Cawston, T. E., Taylor, D. J., DeWitt, D. L., and Saklatvala, J. (1997) Actions of IL-1 are selectively controlled by p38 mitogen-activated protein kinase: Regulation of prostaglandin H synthase-2, metalloproteinases, and IL-6 at different levels. *J. Immunol. 158*, 3165–3173.

(2) Miyazawa, K., Mori, A., Miyata, H., Akahane, M., Ajisawa, Y., and Okudaira, H. (1998) Regulation of interleukin-1β-induced interleukin-6 gene expression in human fibroblast-like synoviocytes by p38 mitogen-activated protein kinase. *J. Biol. Chem. 273*, 24832–24838.

(3) Westra, J., Limburg, P. C., de Boer, P., and van Rijswijk, M. H. (2004) Effects of RWJ 67657, a p38 mitogen activated protein kinase (MAPK) inhibitor, on the production of inflammatory mediators by rheumatoid synovial fibroblasts. *Ann. Rheum. Dis. 63*, 1453–1459.

(4) Han, C., Smolen, J. S., Kavanaugh, A., van der Heijde, D., Braun, J., Westhovens, R., Zhao, N., Rahman, M. U., Baker, D., and Bala, M. (2007) The impact of infliximab treatment on quality of life in patients with inflammatory rheumatic diseases. *Arthritis Res. Ther. 9*, R103.

(5) Cohen, S., Moreland, L., Cush, J., Greenwald, M., Block, S., Shergy, W., Hanrahan, P., Kraishi, M., Patel, A., Sun, G., and Bear, M. (2004) A multicentre, double blind, randomised, placebo controlled trial of anakinra (Kineret), a recombinant interleukin 1 receptor antagonist, in patients with rheumatoid arthritis treated with background methotrexate. *Ann. Rheum. Dis. 63*, 1062–1068.

(6) Kievit, W., Fransen, J., Oerlemans, A., Kuper, H., van der Laar, M., de Rooij, D., De Gendt, C., Ronday, K., Jansen, T., van Oijen, P., Brus, H., Adang, E., and van Riel, P. (2007) The efficacy of anti-TNF in rheumatoid arthritis, a comparison between randomised controlled trials and clinical practice. *Ann. Rheum. Dis. 66*, 1473–1478.

(7) Miyasaka, N. (2009) Adalimumab for the treatment of rheumatoid arthritis. *Expert Rev. Clin. Immunol. 5*, 19–26.

(8) Genovese, M. C., Bathon, J. M., Fleischmann, R. M., Moreland, L. W., Martin, R. W., Whitemore, J. B., Tsuji, W. H., and Leff, J. A. (2005) Longterm safety, efficacy, and radiographic outcome with etanercept treatment in patients with early rheumatoid arthritis. *J. Rheumatol. 32*, 1232–1242.

(9) Schett, G., Zwerina, J., and Firestein, G. (2008) The p38 mitogen activated protein kinase (MAPK) pathway in rheumatoid arthritis. *Ann. Rheum. Dis. 67*, 909–916.

(10) Dodeller, F., and Schulze-Koops, H. (2006) The p38 mitogen-activated protein kinase signaling cascade in CD4 T cells. *Arthritis Res. Ther. 8*, 205.

(11) Choy, E. H. S., and Panayi, G. S. (2001) Cytokine pathways and joint inflammation in rheumatoid arthritis. *N. Engl. J. Med. 344*, 907–916.

(12) Salituro, F. G., Germann, U. A., Wilson, K. P., Bemis, G. W., Fox, T., and Su, M. S. (1999) Inhibitors of p38 MAP kinase: Therapeutic intervention in cytokine-mediated diseases. *Curr. Med. Chem. 6*, 807–823.

(13) Lee, J. C., Kassis, S., Kumar, S., Badger, A., and Adams, J. L. (1999) p38 mitogen-activated protein kinase inhibitors: Mechanisms and therapeutic potentials. *Pharmacol. Ther. 82*, 389–397.

(14) Lee, J. C., Kumar, S., Griswold, D. E., Underwood, D. C., Votta, B. J., and Adams, J. L. (2000) Inhibition of p38 MAP kinase as a therapeutic strategy. *Immunopharmacology 47*, 185–201.

(15) Boehm, J. C., and Adams, J. L. (2000) New inhibitors of p38 kinase. *Expert Opin. Ther. Pat. 10*, 25–37.

(16) Wang, Z., Harkins, P. C., Ulevitch, R. J., Han, J., Cobb, M. H., and Goldsmith, E. J. (1997) The structure of mitogen-activated protein kinase p38 at 2.1-Å resolution. *Proc. Natl. Acad. Sci. U.S.A. 94*, 2327–2332.

(17) Wilson, K. P., Fitzgibbon, M. J., Caron, P. R., Griffith, J. P., Chen, W., McCaffrey, P. G., Chambers, S. P., and Su, M. S. (1996) Crystal structure of p38 mitogen-activated protein kinase. *J. Biol. Chem. 271*, 27696–27700.

(18) Fitzgerald, C. E., Patel, S. B., Becker, J. W., Cameron, P. M., Zaller, D., Pilounis, V. B., O'Keefe, S. J., and Scapin, G. (2003) Structural basis for p38α MAP kinase quinazolinone and pyridol-pyrimidine inhibitor specificity. *Nat. Struct. Biol. 10*, 764–769.

(19) Shewchuk, L., Hassell, A., Wisely, B., Rocque, W., Holmes, W., Veal, J., and Kuyper, L. F. (2000) Binding mode of the 4-anilinoquinazoline class of protein kinase inhibitor: X-ray crystallographic studies of 4-anilinoquinazolines bound to cyclin-dependent kinase 2 and p38 kinase. *J. Med. Chem. 43*, 133–138.

(20) Graneto, M. J., Kurumbail, R. G., Vazquez, M. L., Shieh, H. S., Pawlitz, J. L., Williams, J. M., Stallings, W. C., Geng, L., Naraian, A. S., Koszyk, F. J., Stealey, M. A., Xu, X. D., Weier, R. M., Hanson, G. J., Mourey, R. J., Compton, R. P., Mnich, S. J., Anderson, G. D., Monahan, J. B., and Devraj, R. (2007) Synthesis, crystal structure, and activity of pyrazole-based inhibitors of p38 kinase. *J. Med. Chem. 50*, 5712–5719.

(21) Wang, Z., Canagarajah, B. J., Boehm, J. C., Kassisa, S., Cobb, M. H., Young, P. R., Abdel-Meguid, S., Adams, J. L., and Goldsmith, E. J. (1998) Structural basis of inhibitor selectivity in MAP kinases. *Structure 6*, 1117–1128.

(22) Tong, L., Pav, S., White, D. M., Rogers, S., Crane, K. M., Cywin, C. L., Brown, M. L., and Pargellis, C. A. (1997) A highly specific inhibitor of human p38 MAP kinase binds in the ATP pocket. *Nat. Struct. Biol. 4*, 311–316.

(23) Stelmach, J. E., Liu, L., Patel, S. B., Pivnichny, J. V., Scapin, G., Singh, S., Hop, C. E., Wang, Z., Strauss, J. R., Cameron, P. M., Nichols, E. A., O'Keefe, S. J., O'Neill, E. A., Schmatz, D. M., Schwartz, C. D., Thompson, C. M., Zaller, D. M., and Doherty, J. B. (2003) Design and synthesis of potent, orally bioavailable dihydroquinazolinone inhibitors of p38 MAP kinase. *Bioorg. Med. Chem. Lett. 13*, 277–280.

(24) Trejo, A., Arzeno, H., Browner, M., Chanda, S., Cheng, S., Comer, D. D., Dalrymple, S. A., Dunten, P., Lafargue, J., Lovejoy, B., Freire-Moar, J., Lim, J., McIntosh, J., Miller, J., Papp, E., Reuter, D., Roberts, R., Sanpablo, F., Saunders, J., Song, K., Villasenor, A., Warren, S. D., Welch, M., Weller, P., Whiteley, P. E., Zeng, L., and Goldstein, D. M. (2003) Design and synthesis of 4-azaindoles as inhibitors of p38 MAP kinase. *J. Med. Chem. 46*, 4702–4713.

(25) Goldstein, D. M., Alfredson, T., Bertrand, J., Browner, M. F., Clifford, K., Dalrymple, S. A., Dunn, J., Freire-Moar, J., Harris, S., Labadie, S. S., La Fargue, J., Lapierre, J. M., Larrabee, S., Li, F., Papp, E., McWeeney, D., Ramesha, C., Roberts, R., Rotstein, D., San Pablo, B., Sjogren, E. B., So, O. Y., Talamas, F. X., Tao, W., Trejo, A., Villasenor, A., Welch, M., Welch, T., Weller, P., Whiteley, P. E., Young, K., and Zipfel, S. (2006) Discovery of S-[5-amino-1-(4-fluorophenyl)-1H-pyrazol-4-yl]-[3-(2,3-dihydroxypropoxy)phenyl] methanone (RO3201195), an orally bioavailable and highly selective inhibitor of p38 MAP kinase. *J. Med. Chem. 49*, 1562–1575.

(26) Gill, A. L., Frederickson, M., Cleasby, A., Woodhead, S. J., Carr, M. G., Woodhead, A. J., Walker, M. T., Congreve, M. S., Devine, L. A., Tisi, D., O'Reilly, M., Seavers, L. C. A., Davis, D. J., Curry, J., Anthony, R., Padova, A., Murray, C. W., Carr, R. A. E., and Jhoti, H. (2005) Identification of novel p38α MAP kinase inhibitors using fragment-based lead generation. *J. Med. Chem. 48*, 414–426.

(27) Wrobleski, S. T., and Doweyko, A. M. (2005) Structural comparison of p38 inhibitor-protein complexes: A review of recent p38 inhibitors having unique binding interactions. *Curr. Top. Med. Chem. 5*, 1005–1016.

(28) Natarajan, S. R., and Doherty, J. B. (2005) P38 MAP kinase inhibitors: Evolution of imidazole-based and pyrido-pyrimidin-2-one lead classes. *Curr. Top. Med. Chem. 5*, 987–1003.

(29) Huse, M., and Kuriyan, J. (2002) The conformational plasticity of protein kinases. *Cell 109*, 275–282.

(30) Jacobs, M. D., Caron, P. R., and Hare, B. J. (2008) Classifying protein kinase structures guides use of ligand-selectivity profiles to predict inactive conformations: Structure of lck/imatinib complex. *Proteins 70*, 1451–1460.

(31) Levinson, N. M., Kuchment, O., Shen, K., Young, M. A., Koldobskiy, M., Cole, P. A., and Kuriyan, J. (2006) A Src-like inactive conformation in the abl tyrosine kinase domain. *PLoS Biol. 4*, e144.

(32) Pargellis, C., Tong, L., Churchill, L., Cirillo, P. F., Gilmore, T., Graham, A. G., Grob, P. M., Hickey, E. R., Moss, N., Pav, S., and Regan, J. (2002) Inhibition of p38 MAP kinase by utilizing a novel allosteric binding site. *Nat. Struct. Biol. 9*, 268–272.

(33) Hope, H., Anderson, G., Burnette, B., Compton, R., Devraj, R., Hirsch, J., Jungbluth, G., Kieith, R., Li, X., Mbalaviele, G., Saabye, M., Schindler, J., Selness, S., Sommers, C., Stillwell, L., Venkatraman, N., Webb, E., Zhang, J., and Monahan, J. (2009) Anti-inflammatory properties of a novel N-phenyl pyridinone inhibitor of p38 MAP kinase: Preclinical to clinical translation (manuscript to be submitted for publication).

(34) Burnette, B., Selness, S., Devraj, R., Jungbluth, G., Kurumbail, R. G., Stillwell, L., Anderson, G., Mnich, S., Hirsch, J., Compton, R. P., De Ciechi, P., Hope, H., Hepperle, M., Kieith, R., Naing, W., Shieh, H., Portanova, J., Zhang, Y., Zhang, J., Leimgruber, R., and Monahan, J. (2009) SD-0006: A potent, selective, and orally-available inhibitor of p38 kinase. *Pharmacology* (in press).

(35) Karplus, P. A. (1996) Experimentally observed conformation-dependent geometry and hidden strain in proteins. *Protein Sci. 5*, 1406–1420.

(36) Kleywegt, G. J., and Alwyn, J. T. (1996) Phi/Psi-chology: Ramachandran revisited. *Structure 4*, 1395–1400.

(37) Eyers, P. A., Craxton, M., Morrice, N., Cohen, P., and Goedert, M. (1998) Conversion of SB 203580-insensitive MAP kinase family members to drug-sensitive forms by a singel amino-acid substitution. *Chem. Biol. 5*, 321–328.

(38) Wilson, K. P., McCaffrey, P. G., Hsiao, K., Pazhanisamy, S., Galullo, V., Bemis, G. W., Fitzgibbon, M. J., Caron, P. R., Murcko, M. A., and Su, M. S. (1997) The structural basis for the specificity of pyridinylimidazole inhibitors of p38 MAP kinase. *Chem. Biol. 4*, 423–431.

(39) Lisnock, J., Tebben, A., Frantz, B., O'Neill, E. A., Croft, G., O'Keefe, S. J., Li, B., Hacker, C., de Laszlo, S., Smith, A., Libby, B., Liverton, N., Hermes, J., and LoGrasso, P. (1998) Molecular basis for p38 protein kinase inhibitor specificity. *Biochemistry 37*, 16573–16581.

(40) Manning, G., Whyte, D., Martinez, R., Hunter, T., and Sudarsanam, S. (2002) The protein kinase complement of the human genome. *Science 298*, 1912–1934.

(41) Sullivan, J. E., Holdgate, G. A., Campbell, D., Timms, D., Gerhardt, S., Breed, J., Breeze, A. L., Bermingham, A., Pauptit, R. A., Norman, R. A., Embrey, K. J., Read, J., VanScyoc, W. S., and Ward, W. H. J. (2005) Prevention of MKK6-Dependent Activation by Binding to p38α MAP Kinase. *Biochemistry 44*, 16475–16490.

(42) Mikkelsen, S. S., Jensen, S. B., Chiliveru, S., Melchjorsen, J., Julkunen, I., Gaestel, M., Arthur, J. S. C., Flavell, R. A., Ghosh, S., and Paludan, S. R. (2009) RIG-I-mediated activation of p38 MAPK is essential for viral induction of interferon and activation of dendritic cells. *J. Biol. Chem. 284*, 10774–10782.

(43) Cheung, P. C., Campbell, D., Nebreda, A. R., and Cohen, P. (2003) Feedback control of the protein kinase TAK1 by SAPK2a/p38α. *EMBO J. 22*, 5793–5805.

(44) Heinrichsdorff, J., Luedde, T., Perdiguero, E., Nebreda, A. R., and Pasparakis, M. (2008) p38α MAPK inhibits JNK activation and collaborates with IkB kinase 2 to prevent endotoxin-induced liver failure. *EMBO Rep. 9*, 1048–1054.

(45) Hu, J.-H., Chen, T., Zhuang, Z.-H., Kong, L., Yu, M.-C., Liu, Y., Zang, J.-W., and Ge, B.-X. (2007) Feedback control of MKP-1 expression by p38. *Cell. Signalling 19*, 393–400.